The representation of oral structures in the primary somatosensory cortex and the border region between the secondary somatosensory cortex and insular oral region

Yuki Kirihara

Nihon University Graduate School of Dentistry,

Major in Oral and Maxillofacial Surgery

(Directors: Profs. Morio Tonogi, Masayuki Kobayashi, and Satoshi Fujita)

Index

This thesis is composed of the following article and the additional result showing the degrees of scattered initial responses to electrical stimulation and air puff stimulation (Fig. 2).

Kirihara, Y., Zama, M., Fujita, S., Ogisawa, S., Nishikubo, S., Tonogi, M., & Kobayashi, M. (2022). Asymmetrical organization of oral structures in the primary and secondary somatosensory cortices in rats: An optical imaging study. *Synapse*, 76, e22222. https://doi.org/10.1002/syn.22222

Abstract

In rodents, the representation of the body surface in the primary somatosensory cortex (S1) forms a mirror image along the ventral border of the S1 in the secondary somatosensory cortex (S2). Sensory information from the oral region is processed in the S1 and the border region between the S2 and insular oral region (IOR). The relationship between somatosensory representations in the S1 and S2/IOR was examined using optical imaging with a voltage-sensitive dye in urethane-anesthetized rats. In reference to the rhinal fissure and middle cerebral artery, a somatosensory map was constructed by applying electrical or air puff stimulation. The initial neural excitation in the S1 to facial structures, including the eyebrow, cornea, pinna, whisker pad, nasal tip, and nasal mucosa, spread toward the ventral area, putatively the S2. The initial cortical responses in the S1 to oral structures, including the lower lip, tongue, and teeth, were spatially separated from those in the S2/IOR. The representation of the dorsum of the tongue, tongue tip, mandibular molar pulp, mandibular incisor pulp, and mandibular incisor periodontal ligament were almost linearly arranged from caudal to rostral in both S1 and S2/IOR. The lower lip was represented in the dorsal area from the representation of teeth and tongue in both S1 and S2/IOR. The representations of maxillary teeth were caudodorsal to the representations of mandibular teeth in the S1 and S2/IOR, respectively. These results suggest that the representation of oral structures in the S1 formed a non-mirror image, in the S2/IOR.

Introduction

In rats, somatosensory information from peripheral structures is conveyed to higher brain regions, including somatosensory cortical areas, i.e., the primary somatosensory cortex (S1), the secondary somatosensory cortex (S2), and the parietal ventral area (Benison, Rector, & Barth, 2007; Fabri & Burton, 1991; Harding-Forrester & Feldman, 2018; Remple, Henry, & Catania, 2003). These somatosensory cortical areas have a topographic map corresponding to the body parts (Benison, Rector, & Barth, 2007; Fabri & Burton, 1991; Harding-Forrester & Feldman, 2018; Remple, Henry, & Catania, 2003). In the rodent S1, the representations of body structures from caudal to rostral are arranged from medial to lateral cortical areas: the representations of the face, neck, and body in the S1 are arranged from the rostroventral to caudodorsal cortical areas (Chapin & Lin, 1984; Welker, 1976). The representation of the body surface and the row of whiskers in the S1 forms a smaller mirror image along the ventral border of the S1 in the S2 (Benison, Rector, & Barth, 2007; Harding-Forrester & Feldman, 2018; Hoffer, Hoover, & Alloway, 2003; Hubatz, Hucher, Shulz, & Férézou, 2020).

The trigeminal nerve innervates various facial structures, including the eye, nose, and whiskers (Heaton et al., 2014), in addition to oral structures, such as the tooth pulp, periodontal ligament (PDL), tongue, and gingiva (Bae & Yoshida, 2020, Wakisaka et al., 1985). In terms of oral structures, the S1 areas corresponding to the lower incisor and tongue are located ventrally adjacent to the lower and upper jaws, respectively (Harding-Forrester & Feldman, 2018; Remple, Henry, & Catania, 2003). Remple, Henry, &

Catania, (2003) et al., mapped the somatosensory cortices related to the oral region using an electrophysiological technique. The mandibular incisor is represented in two areas: oral modules (OMs) 1 and 3. In agreement with their study, the following studies conducted using an optical imaging technique with a voltage-sensitive dye (VSD) have revealed that cortical responses to electrical stimulation of the mandibular incisor initiate from two cortical areas—a ventral part of the S1 and the border between the ventral part of S2 and insular cortex (S2/IOR), which correspond to OM1 and OM3, respectively (Horinuki, Shinoda, Shimizu, Koshikawa, & Kobayashi, 2015; Nakamura, Kato, Shirakawa, Koshikawa, & Kobayashi, 2015; Nakamura, Shirakawa, Koshikawa, & Kobayashi, 2016). However, the relationship between the maps of S1 and S2/IOR regarding the oral structures is still limited, although the arrangements and positional relationship between somatosensory maps in the S1 and S2 regarding the body surface are well known.

This study aimed to clarify the topography of the oral structures in the S1 and S2/IOR and to determine whether the oral structures exhibit a cortical representation profile similar to that of the face, neck, limbs, fingers, and trunk, whose representation profiles in the S2 are smaller mirror images of those in the S1. Previous studies suggest that the rhinal fissure (RF) and the middle cerebral artery (MCA) are useful landmarks for the creation of somatosensory maps (Accolla, Bathellier, Petersen, & Carleton, 2007; Kosar, Grill, & Norgren, 1986; Yamamoto, 1984). To increase the accuracy of the relative spatial distribution of activated cortical areas responding to the oral structures, not only oral structures including the lower lip, tongue, and incisor and molar teeth of the

maxilla and mandible but also facial structures including the eyebrow, cornea, pinna, whisker pad, nasal tip, and nasal mucosa were examined. Stimulation was applied in two ways: electrical stimulation via inserted electrodes and air puff stimulation.

Materials and Methods

Animals and surgical procedures for *in vivo* optical imaging

The Animal Experimentation Committee of Nihon University approved the experiments (AP19DEN014–2), and all experiments were performed according to the institutional guidelines for the care and use of experimental animals described in the National Institutes of Health Guide for the Care and Use of Laboratory Animals. All efforts were made to minimize animal suffering and to reduce the number of animals used.

Male Wistar rats (Sankyo Laboratories, Tokyo, Japan) weighing 190 ± 12 g (mean ± SEM; n = 36) were used for optical imaging experiments. The rats were housed in cages (27 × 45 × 20 cm) for approximately 1 week until the experimental day. Food and water were freely available. The temperature (23 ± 2°C) and humidity (55 ± 5%) in the animal room were controlled with a 12 h light/dark cycle (lights on at 0700 h; off at 1900 h). Optical imaging with a VSD (RH-1691, Optical Imaging, New York, NY, USA) was performed as previously described (Fujita, Yamamoto, & Kobayashi, 2019; Nakamura, Kato, Shirakawa, Koshikawa, & Kobayashi, 2015; Noma et al., 2020; Zama, Fujita, Nakaya, Tonogi, & Kobayashi, 2019; Zama, Hara, Fujita, Kaneko, & Kobayashi, 2018). Briefly, the rats received an atropine methyl bromide injection (0.5 mg/kg, i.p.) and were anesthetized with urethane (1.5 g/kg, i.p., Sigma-Aldrich, St. Louis, MO, USA). Anesthesia efficacy was gauged by the toe pinch reflex, and additional urethane was administered as needed. Body temperature was monitored with a rectal probe and was maintained at approximately 37°C with a heating pad (BWT-100, Bio Research Center,

Osaka, Japan). Rats were fixed to a custom-made stereotaxic snout frame, which was tilted 50° laterally for imaging the surface of the left lateral part of the S1 and S2/IOR using a CCD camera (MiCAM02, Brainvision, Tokyo, Japan). The left temporal muscle and zygomatic arch were carefully removed, and a craniotomy was performed to expose the S1 and S2/IOR, including the RF and MCA.

RH-1691 (1 mg/ml) in 0.9% saline was applied to the cortical surface for 1 h. Then, the cortical surface was rinsed with saline and covered with 1% agarose (Agarose Low EEO, Sigma-Aldrich) dissolved in Ringer's solution and affixed with a glass coverslip. RH-1691 fluorescence intensities were measured using the CCD camera system described above, which was mounted on a stereomicroscope (Leica Microsystems, Wetzlar, Germany). The cortical surface was illuminated through a 632 nm excitation filter and a dichroic mirror using a tungsten-halogen lamp (CLS150XD, Leica Microsystems). Fluorescent emission was captured through an absorption filter ($\lambda > 650$ nm longpass, Andover, Salem, MA, USA). The CCD camera had a 6.4 × 4.8 mm^2 imaging area (184 × 124 pixels).

To remove signals resulting from acute bleaching of the dye, values in the absence of any stimuli were subtracted from each recording. Thus, each image was constructed from paired recordings with and without stimulation. The sampling rate was set at 250 Hz (4 ms/frame), and the acquisition time was 300 ms, including baseline (50 ms). Twenty-four consecutive images in response to electrical stimulation and forty consecutive images in response to air puff stimulation were averaged to reduce the noise described above. The intervals between recordings with stimulation were set at 20 s.

Electrical stimulation and air puff stimulation

In this study, rats were divided into the electrical stimulation group (n = 19) and the air puff stimulation group (n = 17) to avoid the possibility that inserted electrode-induced injury might affect somatosensation induced by air puff stimulation. All whiskers, but not other hair, were shaved in both groups.

In the electrical stimulation group, bipolar electrodes made from an enamel-coated copper wire (diameter 80 μm for molar pulp stimulation and 100 μm for skin stimulation; Tamagawadensen, Tokyo, Japan) were inserted into the right skin/mucosa (the eyebrow, whisker pad (C3), lower lip, and tongue), right dental pulp (the maxillary and mandibular incisor and the 1st molars), and right PDL (the maxillary and mandibular incisor). The tip of the wire (0.5–1.0 mm) was bare and fixed with dental cement (Estelite Flow Quick, Tokuyama Dental, Tokyo, Japan). For electrical stimulation, voltage pulses with a 100 μs duration and 5 V amplitude were applied using a stimulator unit (STG2008, Multi Channel Systems, Reutlingen, Germany). In the present study, five voltage pulses at 50 Hz were applied.

In the air puff stimulation group, the tip of a polyethylene tube (inner diameter = 0.5 mm) was placed approximately 1 mm from the right eyebrow, cornea, pinna (medial surface), whisker pad (C3), tip of the nose (nasal tip), and lower lip. To stimulate the nasal mucosa, a polyethylene tube was inserted 1 mm into the right nostril. An artificial tear eye drop (Soft Santear, Santen, Osaka, Japan) was applied to the cornea at intervals

of 1 hr until the cornea recordings were carried out. The air temperature was kept at room temperature (20–25°C). The air puff was applied with air pressure at 5 psi (cornea) or 20 psi (other regions). Cortical responses to the air puff (100 ms) were recorded from the left cortex through the use of VSD imaging as mentioned above.

Data analysis

Optical imaging data were processed and analyzed using Brain Vision Analyzer software (Brainvision). Changes in the intensity of fluorescence (ΔF) of each pixel relative to the initial intensity of fluorescence (F) were calculated ($\Delta F/F$), and the ratio was processed with a spatial filter (9 × 9 pixels). A significant response was defined as a signal exceeding 7 times the SD in the baseline recording period. To compare cortical responses, images were aligned across multiple rats using the RF and intersection of RF and MCA as landmarks. In some of the images, the image was grafted with a captured background image. Locations of the initial responses were marked at the center position in the first frame that exhibited a significant increase in the optical signal. A region of interest (ROI) was a circle consisting of 77 pixels (~ 0.1 mm^2). In this study, some of the responses showed dull, not sharp, peaks (Fig. 1Ab, Bb). To evaluate maximum responses, the frames in which the optical signal exceeded 95% of the maximum amplitude in the center of the initial response in the S1 were used. It was difficult to discriminate initial responses in the S2 from spread neural excitation from the S1 in the cases of the eyebrow, cornea, pinna, whisker pad, nasal tip, and nasal mucosa. Therefore, only initial S1 responses were assessed in these cases. On the other hand, the initial responses in the S1

and S2/IOR were clearly separated in the cases of the lower lip, tongue, and teeth, and therefore, each initial response in the S1 and S2/IOR was assessed. The latency was defined as the time elapsed between the onset of stimulation and the time at which a significant optical response was first detected.

In comparison of the degrees of scattered initial responses between electrical stimulation and air puff stimulation, the distance from the averaged initial response to each initial response was defined as the gap.

In 4% of rats, the MCA exhibited angioplany, e.g., the bifurcation at the rhinal fissure. In these animals, the rhinal fissure and the MCA could not be aligned with those of the other animals, and therefore, the results obtained from these animals were excluded.

The data are expressed as the mean ± SEM. To compare latency between the S1 and S2/IOR, paired *t* test or Wilcoxon signed-rank test was used in accordance with the results of the normality test (Shapiro–Wilk test). To compare the latency and gap, either Student's *t* test or Mann–Whitney *U* test was used in accordance with the results of the normality test (Shapiro–Wilk test) and equal variance test (Brown–Forsythe test). $p < 0.05$ was considered significant.

Results

Activation of the S1 via stimulation of the facial structures

Typical examples of responses to electrical stimulation and air puff stimulation of the eyebrow are shown in Fig. 1A, B. Neural excitation initially spread from the initial response in a concentric manner (Fig. 1A, circle, arrowhead). Subsequently, neural excitation spread in the ventral direction, putatively to part of the S2. Finally, neural excitation appeared in the rostroventral area from the initial response. In the case of air puff stimulation of the eyebrow, the initial response was observed in a similar area (Fig. 1B, circle, arrowhead). Similarly, neural excitation spread from the initial response in a concentric manner and then spread ventrally. Compared to the optical response to electrical stimulation in the ROI of the initial response, the optical response to air puff stimulation showed a longer delay from the onset of stimulation and a longer peak response (Fig. 1Bb, arrow). A longer latency of the air puff stimulation-induced cortical responses than of the electrical stimulation-induced cortical responses was observed in the other parts of stimulation (Table 1).

Fig. 1C shows superimposed images of the initial (open circles) and maximum responses to electrical stimulation of the eyebrow (gray patches) obtained from 15 rats (right panel) with examples of initial and maximum responses on the left panels. To visualize the spatial distribution patterns, each initial and maximum response was superimposed with the RF and MCA as references (Fig. 1C, right panel). The majority of initial responses to the air puff stimulation of the eyebrow (Fig. 1D, K) were also found

in areas corresponding to the initial responses to the electrical stimulation of the eyebrow, whereas a part of initial responses was scattered in the ventral areas.

The averaged initial response to the air puff stimulation of the cornea was located at the rostroventral area from the initial response to electrical stimulation of the eyebrow (Fig. 1E, K). However, each initial response to air puff stimulation of the cornea was broadly scattered; the initial responses in 5 cases were observed in the area close to the averaged initial responses to the electrical stimulation of the eyebrow, whereas the initial responses in 6 cases were found in the area around the nose region, which is referred to hereinafter (Fig. 1K).

The averaged initial response to the air puff stimulation of the pinna was also observed in the area close to the initial response to the electrical stimulation of the eyebrow (Fig. 1F, K).

The areas in response to the nose region, such as the whisker pad, nasal tip, and nasal mucosa within the S1 somatotopic map, were also examined. In response to the electrical and air puff stimulations of the whisker pad, the cortical excitation spread from the initial response in a concentric manner and slightly spread toward the ventral area (Fig. 1G, H). The averaged initial responses to electrical and air puff stimulation of the whisker pad were closely located (Fig. 1G, H, K), although each initial response induced by the electrical stimulation was more compactly located than that induced by the air puff stimulation (Fig. 1G, H). The gaps between averaged initial response to the eyebrow stimulation and each initial response were 0.63 ± 0.09 mm in electrical stimulation (n =

15) and 1.78 ± 0.30 mm in air puff stimulation (n = 10, $p < 0.001$, Mann–Whitney U test, Fig. 2A).

The gaps between averaged initial response and each initial response to the whisker stimulation were 0.82 ± 0.11 mm in electrical stimulation (n = 17) and 1.46 ± 0.15 mm in air puff stimulation (n = 13, $p = 0.002$, Student's t test, Fig. 2B).

In examination of the nasal tip and nasal mucosa (Fig. 1I-K), cortical responses were found in a similar fashion in the whisker pad. Although stimulation of the nasal tip and nasal mucosa was performed with air puff stimulation, each initial response showed a small spatial variation. The averaged initial response to the nasal tip was located caudally to that to the nasal mucosa, in agreement with previous study (Zama, Hara, Fujita, Kaneko, & Kobayashi, 2018).

Activation of the S1 and S2/IOR via stimulation of the oral structures

Unlike the cortical responses to the stimulations of the eye and nose regions, the cortical responses to the stimulations of the oral structures such as lower lip, tongue, and teeth were clearly initiated from two separated areas, the S1 and S2/IOR (Fig. 3). Therefore, cortical responses in both the S1 and S2/IOR were quantified in the following analyses.

Compared to the cortical responses to other oral structures, the cortical responses to the lower lip were initiated from relatively dorsal areas in the S1 and S2/IOR (Fig. 3A, B). The neural excitations spread from each initial responding area in a concentric manner in both S1 and S2/IOR. The averaged initial responses to electrical and air puff stimulation of the lower lip were found in the close sites in both the S1 and S2/IOR (Fig. 3A, B, K).

Each initial response was compactly located except for in some cases of air puff stimulation. The gaps between averaged initial response and each initial response were 0.51 ± 0.07 mm in electrical stimulation (n = 14) and 0.81 ± 0.14 mm in air puff stimulation (n = 10, p = 0.07, Student's t test) in the S1, whereas the gaps between averaged initial response and each initial response were 0.37 ± 0.06 mm in electrical stimulation and 0.71 ± 0.17 mm in air puff stimulation (p = 0.095, Mann–Whitney U test, Fig. 2C) in the S2/IOR.

In the electrical stimulation of the tongue, the stimulation electrodes were inserted into the tip (Fig. 3C) and middle part of the tongue (dorsum of the tongue; Fig. 3D). Electrical stimulation of the tongue induced cortical responses in both the S1 and S2/IOR (Fig. 3C, D). The averaged initial responses to the tongue tip were located rostral to those responding to the middle part of the tongue in both S1 and S2/IOR (Fig. 3K). This arrangement of the tongue in S1 agrees with a previous study (Remple, Henry, & Catania, 2003). In addition, the latency between the tongue tip and dorsum of the tongue was compared (Table 1). Latency in the tongue tip was significantly shorter than that in the dorsum of the tongue in both the S1 (tongue tip, 21.7 ± 2.1 ms, n = 14; dorsum of the tongue , 50.6 ± 7.0 ms, n = 7; p = 0.002, Mann-Whitney U test) and S2/IOR (tongue tip, 29.4 ± 3.5 ms; dorsum of the tongue, 54.0 ± 8.8 ms; p = 0.012, Mann-Whitney U test).

Activation of the S1 and S2/IOR via stimulation of the incisor and molar

The cortical responses to electrical stimulation of the mandibular and maxillary incisor and molar pulps and PDLs (Fig. 3L) were also examined. As shown in Fig. 3E-G,

electrical stimulation of the mandibular teeth induced clear cortical responses in both the S1 and S2/IOR.

In the S1, the averaged initial response to electrical stimulation of the mandibular incisor PDL was found in the most rostral part of the S1 in this study. This activated area almost overlapped with the averaged initial response to electrical stimulation of the mandibular incisor pulp (Fig. 3E, G). The averaged initial response to electrical stimulation of the mandibular molar pulp was slightly caudal to that of the mandibular incisor (Fig. 3K). In the S2/IOR, the rostrocaudal arrangement of averaged initial responses to electrical stimulations of the incisors and molars of the mandibula was the same as that in the S1 (Fig. 3K).

Regarding the electrical stimulation of the maxillary teeth, the cortical responses in the S1 were faint and scattered, whereas the cortical response in the S2/IOR was rather consistent (Fig. 3H-J). In the S1, the averaged initial responses to the electrical stimulations of the maxillary molar pulp (Fig. 3H), the maxillary incisor pulp (Fig. 3I), and the maxillary incisor PDL (Fig. 3J) were found in the area caudal to the initial responses of mandibular teeth (Fig. 3K, 13-15). On the other hand, in the S2/IOR, the averaged initial responses in the maxillary teeth (Fig. 3K, 16-18) were found in the area dorsal to the initial responses of mandibular teeth (Fig. 3K, 13-15).

Spatial topography of the averaged initial responses to orofacial structures

A summary of the initial responses is shown in Fig. 4. The averaged initial responses to dorsum of the tongue (12), tongue tip (11), mandibular molar pulp (13), mandibular

incisor pulp (14), and mandibular incisor PDL (15) were almost linearly arranged from caudal to rostral in the S1. The arrangement from caudal to rostral in the S2/IOR was the same as that in the S1. The representation of maxillary teeth was caudal to the representation of mandibular teeth in the S1, whereas the representation of maxillary teeth was dorsal to the representation of mandibular teeth in the S2/IOR. The lower lip (9) was represented in the dorsal area from the representation of teeth and tongue in both the S1 and S2/IOR.

Discussion

The present study demonstrated the somatosensory map of orofacial structures in the S1 and S2/IOR in reference to the RF and MCA as landmarks. It is well known that the representation of the body surface, including regions of the head, forms a mirror image of the S1 corresponding to the S2 (Benison, Rector, & Barth, 2007; Harding-Forrester & Feldman, 2018; Hoffer, Hoover, & Alloway, 2003; Hubatz, Hucher, Shulz, & Férézou, 2020). In contrast, the present study demonstrated the different manner of representation of oral structures compared to face and body structures in the S2/IOR: the representation in the S2/IOR was a parallel shift image of the S1, not a mirror image of that in the S1.

Technical consideration of electrical and air puff stimulation

Electrical stimulation via electrodes is a potent method to visualize cortical responses to somatosensory stimulation in VSD imaging experiments because the stimulus onset is completely controlled. However, it is difficult to place electrodes in some regions, e.g., the pinna, cornea, nasal mucosa, and nasal tip. Electrical stimulation is likely to activate most afferents, including Aβ, Aδ, and C fibers (Kaneko, Horinuki, Shimizu, & Kobayashi, 2017). The cortical responses might reflect not only touch and pressure but also nociception, which might affect cortical responses induced by electrical stimulation. Therefore, air puff stimulation was additionally used as an alternative method to evoke intrinsic somatosensory stimulation in addition to electrical stimulation in the present study.

Electrical stimulation-induced initial responses were observed in a smaller area than air puff stimulation-induced initial responses. This may be due to the large size of the stimulated area. The diffusion of puffed air should be taken into consideration. For example, air puff applied to the nasal mucosa must be diffused to the upper pharynx (Zama, Hara, Fujita, Kaneko, & Kobayashi, 2018). Although some initial responses were observed far from other initial responses in air puff stimulation, the area of initial responses almost overlapped in the comparison between electrical stimulation and air puff stimulation. Thus, air puff stimulation is more suitable than electrical stimulation for the application of physiological stimuli; however, the accuracy of mapping to identify the cortical region responding to some peripheral structures is limited (Fig. 2).

In cortical responses to electrical stimulation of the tongue, latency in the tongue tip was significantly shorter than that in the dorsum of the tongue in both the S1 and S2/IOR. In human, the sensitivity at the dorsum of the tongue is lower compared to that at the tip of tongue (Pamir, Z., Canoluk, M.U., Jung, J.H., & Peli, E. 2020). If this is the case in rats, the different latency might reflect the different sensitivities based on the part of tongue. This possibility should be addressed in the future study.

The initial responses to air puff stimulation of the cornea were observed in two areas: the area close to the representation of the eyebrow and the area close to the representation of the whisker pad, nasal tip, and nasal mucosa (Fig. 1E, K). The enhanced excitability in a rat model of dry eye is characterized by enlarged convergent receptive fields from periorbital skin, including whisker pads and nose tips, consistent with central sensitization (Rahman, Okamoto, Thompson, Katagiri, & Bereiter, 2015). Therefore,

repeated air puff stimulation might damage the cornea and possibly induce cortical responses initiated from the area close to the representation of the whisker pad, nasal tip, and nasal mucosa.

Reliability of the references, RF and MCA, of the sensory map

Previous studies suggest that the RF and MCA are useful landmarks to make somatosensory maps in the lateral cortical areas (Accolla, Bathellier, Petersen, & Carleton, 2007; Kosar, Grill, & Norgren, 1986; Yamamoto, 1984). On the other hand, it has been reported that there are many individual differences in the traverses of the MCA (McDaniel & Tucker, 1992). In 4% of rats, highly individual traverses of the MCA were found, in which the MCA was bifurcated in an area ventral to the RF (Nakamura, Kato, Shirakawa, Koshikawa, & Kobayashi, 2015). In such cases, the MCA cannot be aligned with those of other animals. In the present study, the RF and the intersection of the RF and MCA, but not the angle of the MCA and branching, were utilized as landmarks. To confirm the validity of the landmarks, cortical responses to somatosensory stimulations in not only oral structures but also other facial structures represented in areas far from the RF were obtained. If the landmarks had high individual differences, the obtained initial responses would show highly scattered plots on the map to emphasize the individual differences. As a result, the cortical responses to electrical stimulation of the eyebrow and air puff stimulations of the nasal tip and nasal mucosa were observed with the same accuracy as the oral region representing areas close to the RF. These results suggested

that the representation of the oral region in the S1 and S2/IOR was precisely obtained using the RF and the intersection of RF and MCA as landmarks.

Precise representation profiles of the maxillary teeth in the S1 and S2/IOR

Remple, Henry, & Catania (2003) demonstrated that the mandibular incisor stimulated by small probes and calibrated von Frey hairs represents two somatosensory areas, OM1 and OM3, which corresponded to the S1 and S2/IOR, respectively, in following study using optical imaging with a VSD (Nakamura, Kato, Shirakawa, Koshikawa, & Kobayashi, 2015). The representation of the maxillary incisor overlaps with that of the mandibular incisor in the OM3, whereas the representation of the maxillary incisor in the S1 is illustrated in the area caudal to the representation of the tongue and adjacent to the OM3. On the other hand, the averaged initial responses to the maxillary incisor and molar were observed in the area between the mandibular teeth and tongue in the S1 in this study (Fig. 4). In addition to the mandibular incisor, it has been reported that the cortical responses to stimulation of the oral region, such as the mentum, tongue, dental pulp and PDL of the maxillary incisor and 1st molar, are separate in both the S1 and S2/IOR (Fujita, Yamamoto, & Kobayashi, 2019; Horinuki, Shinoda, Shimizu, Koshikawa, & Kobayashi, 2015; Horinuki, Yamamoto, Shimizu, Koshikawa, & Kobayashi 2016; Kaneko, Fujita, Shimizu, Motoyoshi, & Kobayashi, 2018; Kaneko, Horinuki, Shimizu, & Kobayashi, 2017; Kobayashi & Horinuki, 2017; Nakamura, Kato, Shirakawa, Koshikawa, & Kobayashi, 2015; Noma et al., 2020; Zama, Fujita, Nakaya, Tonogi, & Kobayashi, 2019). Among them, the cortical responses to the electrical stimulations of the dental pulp and

PDL in the maxillary incisor and molar were faint in the S1 and consistent in the S2/IOR. Indeed, the latency of maxillary molar pulp was significantly longer in the S1 than that in the S2/IOR (Table 1), which might be due to smaller responses in the S1. These findings suggest that the faint cortical responses in the S1 could be undetectable for the multiunit recording and may be a part of the reason that the S1 corresponding to the maxillary incisor was described to be adjacent to the OM3 in Remple's study (2003).

The faint excitation pattern in the S1 may raise the question of whether the faint cortical responses in the S1 to maxillary tooth stimulation are just artifacts or true signals. The S1 responses to stimulation of the maxillary teeth become apparent under specific experimental conditions. In a rat ectopic pain model, inferior alveolar nerve transection induces enhancement of cortical responses to electrical stimulation of the maxillary molar pulp in both the S1 and S2/IOR (Fujita, Yamamoto, & Kobayashi, 2019). The enhanced cortical excitation propagates in a concentric manner from each initial response in the S1 and S2/IOR. Similarly, cortical responses to electrical stimulation of the maxillary molar PDL in the S1 are clearly found in rat models of orthodontic tooth movement (Horinuki, Shinoda, Shimizu, Koshikawa, & Kobayashi, 2015; Horinuki, Yamamoto, Shimizu, Koshikawa, & Kobayashi 2016; Kobayashi & Horinuki, 2017). In addition to such pain models, mechanical stimulation of the maxillary incisor and molar, in which teeth are ligated with a wire and are pulled by a motor unit, induces substantial cortical responses in the S1 (Kaneko, Fujita, Shimizu, Motoyoshi, & Kobayashi, 2018; Kaneko, Horinuki, Shimizu, & Kobayashi, 2017). Thus, somatosensory information from the maxillary teeth could be processed not only in the S2/IOR but also in the S1.

The map of oral structures shows a specific topographic profile of the S1 and S2/IOR

It is well known that the representation of the body surface in the S1 forms a smaller and symmetric mirror image in the S2 (Benison, Rector, & Barth, 2007; Harding-Forrester & Feldman, 2018; Hoffer, Hoover, & Alloway, 2003). In this study, reliable cortical responses to electrical stimulation of the tongue tip, middle tongue, mandibular molar pulp, mandibular incisor pulp, and mandibular incisor PDL were obtained in both the S1 and S2/IOR. The averaged initial responses in the S1 and S2/IOR are shown in Fig. 4A (green polygons), which formed a rough triangle with vertices of the lower lip, dorsum of the tongue , and mandibular incisor PDL. The triangle in the S2/IOR was smaller than that in the S1, which is a common feature in the representation of the body surface in the S1 and S2 (Benison, Rector, & Barth, 2007; Harding-Forrester & Feldman, 2018; Hoffer, Hoover, & Alloway, 2003). On the other hand, another feature, a symmetric mirror image, was not an applicable rule for the representation of the oral region in the S1 and S2/IOR. If the representation of oral structures in the S1 formed a mirror image in the S2/IOR, the triangle in the S1 would be inverted in the S2/IOR. However, the arrangements of vertices of the lower lip in the dorsal area, mandibular incisor PDL in the rostral area, and dorsum of the tongue in the caudal area were the same in both the S1 and S2/IOR. These results suggest that the representation of oral structures in the S1 formed a parallel shift image, but not a mirror image, in the S2/IOR.

Acknowledgements

I am grateful to Prof. Morio Tonogi for the opportunity to perform this study, Profs. Masayuki Kobayashi and Satoshi Fujita for their instructions of this study, and colleagues in Department of Pharmacology for their technical advice and assistance.

References

Accolla, R., Bathellier, B., Petersen, C.C., & Carleton, A. (2007). Differential spatial representation of taste modalities in the rat gustatory cortex. *The Journal of Neuroscience*, 27(6), 1396-1404. https://doi.org/10.1523/JNEUROSCI.5188-06.2007.

Bae, Y.C., & Yoshida, A. (2020). Morphological foundations of pain processing in dental pulp. *Journal of Oral Science*, 62(2), 126-130. https://doi.org/10.2334/josnusd.19-0451.

Benison, A.M., Rector, D.M., & Barth, D.S. (2007). Hemispheric mapping of secondary somatosensory cortex in the rat. *Journal of Neurophysiology*, 97(1), 200-207. https://doi.org/10.1152/jn.00673.2006.

Chapin, J.K., & Lin, C.S. (1984). Mapping the body representation in the SI cortex of anesthetized and awake rats. *The Journal of Comparative Neurology*, 229(2), 199-213. https://doi.org/10.1002/cne.902290206.

Fabri, M., & Burton, H. (1991). Ipsilateral cortical connections of primary somatic sensory cortex in rats. *The Journal of Comparative Neurology*, 311(3), 405-424. https://doi.org/10.1002/cne.903110310.

Fujita, S., Yamamoto, K., & Kobayashi, M. (2019). Trigeminal nerve transection-induced neuroplastic changes in the somatosensory and insular cortices in a rat ectopic pain model. *eNeuro*, 6(1), ENEURO.0462-18.2019. https://doi.org/10.1523/ENEURO.0462-18.2019.

Harding-Forrester, S., & Feldman, D.E. (2018). Somatosensory maps. *Handbook of Clinical Neurology*, 151, 73-102. https://doi.org/10.1016/B978-0-444-63622-5.00004-8.

Heaton, J.T., Sheu, S.H., Hohman, M.H., Knox, C.J., Weinberg, J.S., Kleiss, I.J., & Hadlock, T.A. (2014). Rat whisker movement after facial nerve lesion: evidence for autonomic contraction of skeletal muscle. *Neuroscience*, 265, 9-20. https://doi.org/10.1016/j.neuroscience.2014.01.038.

Hoffer, Z.S., Hoover, J.E., & Alloway, K.D. (2003). Sensorimotor corticocortical projections from rat barrel cortex have an anisotropic organization that facilitates integration of inputs from whiskers in the same row. *The Journal of Comparative Neurology*, 466(4), 525-544. https://doi.org/10.1002/cne.10895.

Horinuki, E., Shinoda, M., Shimizu, N., Koshikawa, N., & Kobayashi, M. (2015). Orthodontic force facilitates cortical responses to periodontal stimulation. *Journal of Dental Research*, 94(8), 1158-1166. https://doi.org/10.1177/0022034515586543.

Horinuki, E., Yamamoto, K., Shimizu, N., Koshikawa, N., & Kobayashi, M. (2016). Sequential changes in cortical excitation during orthodontic treatment. *Journal of Dental Research*, 95(8), 897-905. https://doi.org/10.1177/0022034516641276.

Hubatz, S., Hucher, G., Shulz, D.E., & Férézou, I. (2020). Spatiotemporal properties of whisker-evoked tactile responses in the mouse secondary somatosensory cortex. *Scientific Reports,* 10(1), 763. https://doi.org/10.1038/s41598-020-57684-6.

Kaneko, M., Fujita, S., Shimizu, N., Motoyoshi, M., & Kobayashi, M. (2018). Experimental tooth movement temporally changes neural excitation and topographical

map in rat somatosensory cortex. *Brain Research*, 1698, 62-69. https://doi.org/10.1016/j.brainres.2018.06.022.

Kaneko, M., Horinuki, E., Shimizu, N., & Kobayashi, M. (2017). Physiological profiles of cortical responses to mechanical stimulation of the tooth in the rat: An optical imaging study. *Neuroscience*, 358, 170-180. https://doi.org/10.1016/j.neuroscience.2017.06.042.

Kobayashi, M., & Horinuki, E. (2017). Neural mechanisms of nociception during orthodontic treatment. *Journal of Oral Science*, 59(2), 167-171. https://doi.org/10.2334/josnusd.16-0847.

Kosar, E., Grill, H.J., & Norgren, R. (1986). Gustatory cortex in the rat. I. Physiological properties and cytoarchitecture. *Brain Research*, 379(2), 329-341. https://doi.org/10.1016/0006-8993(86)90787-0.

McDaniel, W.F., & Tucker, J.C. (1992). A rapid technique for visualizing cerebral arteries in rat. *Behavioral and Neural Biology*, 58(3), 242-244. https://doi.org/10.1016/0163-1047(92)90552-f.

Nakamura, H., Kato, R., Shirakawa, T., Koshikawa, N., & Kobayashi, M. (2015). Spatiotemporal profiles of dental pulp nociception in rat cerebral cortex: an optical imaging study. *The Journal of Comparative Neurology*, 523(8), 1162-1174. https://doi.org/10.1002/cne.23692.

Nakamura, H., Shirakawa, T., Koshikawa, N., & Kobayashi, M. (2016). Distinct excitation to pulpal stimuli between somatosensory and insular cortices. *Journal of Dental Research*, 95(2), 180-187. https://doi.org/10.1177/0022034515611047.

Noma, D., Fujita, S., Zama, M., Mayahara, K., Motoyoshi, M., & Kobayashi, M. (2020). Application of oxytocin with low-level laser irradiation suppresses the facilitation of cortical excitability by partial ligation of the infraorbital nerve in rats: An optical imaging study. *Brain Research*, 1728, 146588. https://doi.org/10.1016/j.brainres.2019.146588.

Pamir, Z., Canoluk, M.U., Jung, J.H., & Peli, E. (2020). Poor resolution at the back of the tongue is the bottleneck for spatial pattern recognition. *Scientific Reports*, 10(1), 2435. https://doi.org/10.1038/s41598-020-59102-3.

Rahman, M., Okamoto, K., Thompson, R., Katagiri, A., & Bereiter, D.A. (2015). Sensitization of trigeminal brainstem pathways in a model for tear deficient dry eye. *Pain*, 156(5), 942-950. https://doi.org/10.1097/j.pain.0000000000000135.

Remple, M.S., Henry, E.C., & Catania, K.C. (2003). Organization of somatosensory cortex in the laboratory rat (Rattus norvegicus): Evidence for two lateral areas joined at the representation of the teeth. *The Journal of Comparative Neurology*, 467(1), 105-118. https://doi.org/10.1002/cne.10909.

Wakisaka, S., Nishikawa, S., Ichikawa, H., Matsuo, S., Takano, Y., & Akai, M. (1985). The distribution and origin of substance P-like immunoreactivity in the rat molar pulp and periodontal tissues. *Archives of Oral Biology*, 30(11-12), 813-818. https://doi.org/10.1016/0003-9969(85)90136-0.

Welker, C. (1976). Receptive fields of barrels in the somatosensory neocortex of the rat. *The Journal of Comparative Neurology*, 166(2), 173-189. https://doi.org/10.1002/cne.901660205.

Yamamoto, T. (1984). Taste responses of cortical neurons. *Progress in Neurobiology*, 23(4), 273-315. https://doi.org/10.1016/0301-0082(84)90007-8.

Zama, M., Fujita, S., Nakaya, Y., Tonogi, M., & Kobayashi, M. (2019). Preceding administration of minocycline suppresses plastic changes in cortical excitatory propagation in the model rat with partial infraorbital nerve ligation. *Frontiers in Neurology*, 10, 1150. https://doi.org/10.3389/fneur.2019.01150.

Zama, M., Hara, Y., Fujita, S., Kaneko, T., & Kobayashi, M. (2018). Somatotopic organization and temporal characteristics of cerebrocortical excitation in response to nasal mucosa stimulation with and without an odor in the rat: An optical imaging study. *Neuroscience*, 377, 77-86. https://doi.org/10.1016/j.neuroscience.2018.02.042.

Table

Table 1. Latency of cortical responses induced by electrical stimulation and/or air puff stimulation in the S1 and S2/IOR

	electrical stimulation		air puff stimulation	
	S1	S2/IOR	S1	S2/IOR
eyebrow	20.7 ± 2.6 (15)	-	54.4 ± 10.4 (10)	-
cornea	-	-	62.7 ± 10.3 (11)	-
pinna	-	-	84.7 ± 28.0 (3)	-
whisker pad	13.3 ± 0.6 (17)	-	37.1 ± 6.6 (13)	-
nasal tip	-	-	32.2 ± 6.0 (11)	-
nasal mucosa	-	-	47.0 ± 4.5 (8)	-
lower lip	17.4 ± 2.8 (14)	20.6 ± 2.4 (14)*	36.8 ± 4.9 (10)	36.4 ± 7.4 (10)
tongue tip	21.7 ± 2.1 (14)	29.4 ± 3.5 (14)*	-	-
dorsum of the tongue	50.6 ± 7.0 (7)	54.0 ± 8.8 (7)	-	-
mandibular molar pulp	34.8 ± 11.9 (10)	23.2 ± 7.1 (10)	-	-
mandibular incisor pulp	20.5 ± 3.0 (8)	16.0 ± 0.7 (8)	-	-
mandibular incisor PDL	23.6 ± 4.2 (5)	18.8 ± 1.8 (5)	-	-
maxillary molar pulp	37.0 ± 6.8 (8)	23.0 ± 4.2 (8)$^{\#}$	-	-
maxillary incisor pulp	30.0 ± 6.2 (4)	29.0 ± 4.8 (4)	-	-
maxillary incisor PDL	59.0 ± 26.3 (4)	20.0 ± 1.7 (4)	-	-

Values indicate mean ± SEM (ms), -: not investigated.

The numbers of animals are shown in parenthesis.

* $p < 0.05$ (vs. S1, paired *t* test), $^{\#}$ $p < 0.05$ (vs. S1, Wilcoxon signed-rank test)

Figures

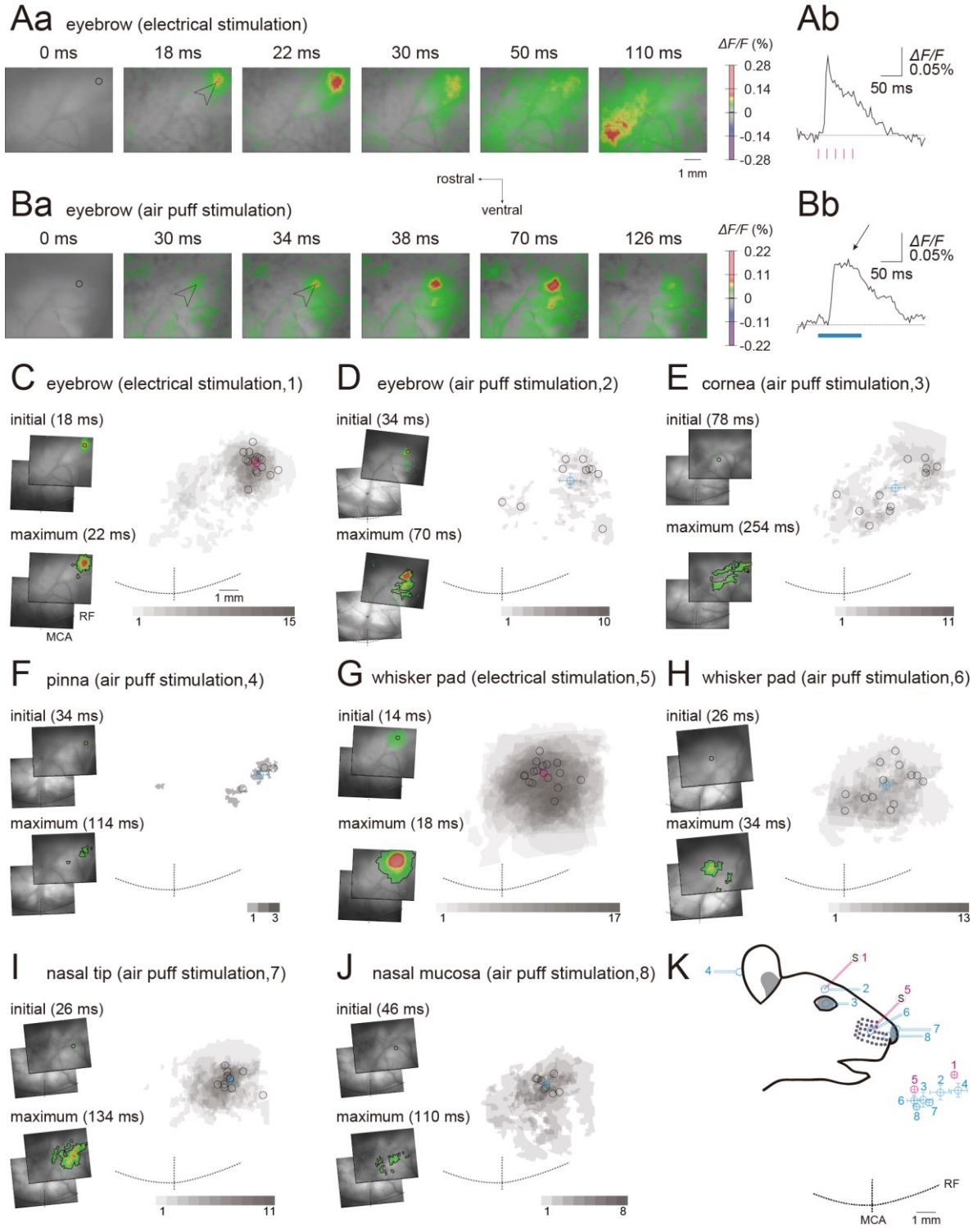
Aa eyebrow (electrical stimulation)
0 ms
18 ms
22 ms
30 ms
50 ms
110 ms
ΔF/F (%)
0.28
0.14
0
-0.14
-0.28
1 mm
rostral
ventral
Ab
ΔF/F 0.05%
50 ms
Ba eyebrow (air puff stimulation)
0 ms
30 ms
34 ms
38 ms
70 ms
126 ms
ΔF/F (%)
0.22
0.11
0
-0.11
-0.22
Bb
ΔF/F 0.05%
50 ms
C eyebrow (electrical stimulation,1)
initial (18 ms)
maximum (22 ms)
RF
MCA
1 mm
1
15
D eyebrow (air puff stimulation,2)
initial (34 ms)
maximum (70 ms)
1
10
E cornea (air puff stimulation,3)
initial (78 ms)
maximum (254 ms)
1
11
F pinna (air puff stimulation,4)
initial (34 ms)
maximum (114 ms)
1
3
G whisker pad (electrical stimulation,5)
initial (14 ms)
maximum (18 ms)
1
17
H whisker pad (air puff stimulation,6)
initial (26 ms)
maximum (34 ms)
1
13
I nasal tip (air puff stimulation,7)
initial (26 ms)
maximum (134 ms)
1
11
J nasal mucosa (air puff stimulation,8)
initial (46 ms)
maximum (110 ms)
1
8
K
S
RF
MCA
1 mm

Figure 1. Cortical responses to electrical stimulation and/or air puff stimulation of the facial structures. (A) An example of excitatory propagation elicited by electrical stimulation of the eyebrow. In Aa, the amplitude of the optical signal (*ΔF/F*) is color-coded, and the time from the onset of electrical stimulation is shown at the top of each panel. Note that the initial excitation in the S1 (black circle and arrowhead) was elicited and spread ventrally. In this case, neural excitation also spread to rostroventral areas in the later phase. In Ab, the temporal profile of optical signals in the regions of interest (ROIs) are indicated by a black circle in Aa. Vertical magenta lines indicate timings of electrical stimuli. (B) An example of spatial (Ba) and temporal (Bb) profiles of excitatory propagation elicited by air puff stimulation of the eyebrow. Note that the initial neural excitation in S1 (black circle and arrowhead) was elicited and spread ventrally. The cyan bar in Bb indicates the period of air puff stimulation (100 ms, 20 psi). (C) Cortical responses to electrical stimulation of the eyebrow. An example of initial and maximum responses is shown in the left panels. The time from the onset of stimulation is shown in parenthesis. The grafted images were aligned across multiple rats using the rhinal fissure (RF) and the intersection of RF and middle cerebral artery (MCA) as landmarks in the right panel (n = 15). Black circles indicate initial responses. The magenta circle with vertical and horizontal bars indicates the location of averaged initial responses and standard error of the mean (SEM) of dorsoventral and rostrocaudal axes, respectively. The number of overlapping maximum responses is represented by the density of color. (D-J) Typical examples of initial and maximum responses to air puff stimulation of the eyebrow (D), air puff stimulation of the cornea (E), air puff stimulation of the pinna (F), electrical stimulation of the whisker pad (G), air puff stimulation of the whisker pad (H), air puff stimulation of the nasal tip (I), and air puff stimulation of the nasal mucosa (J) are shown in the left panel in each panel. The initial and maximum responses are superimposed in the right panel in each panel. The magenta (electrical stimulation) or cyan (air puff stimulation) circles and the bars indicate the location of averaged initial responses and SEM, respectively. Each n value is indicated in the scale bar of the density of color. Note that the initial responses in the cornea were found in primarily two separated areas. (K) Averaged initial responses in S1 are superimposed using the RF and MCA as references. The numbers correspond to stimulated regions and stimulation methods (C-J, inset). Inset: A schema of stimulated regions and the stimulation methods is shown.

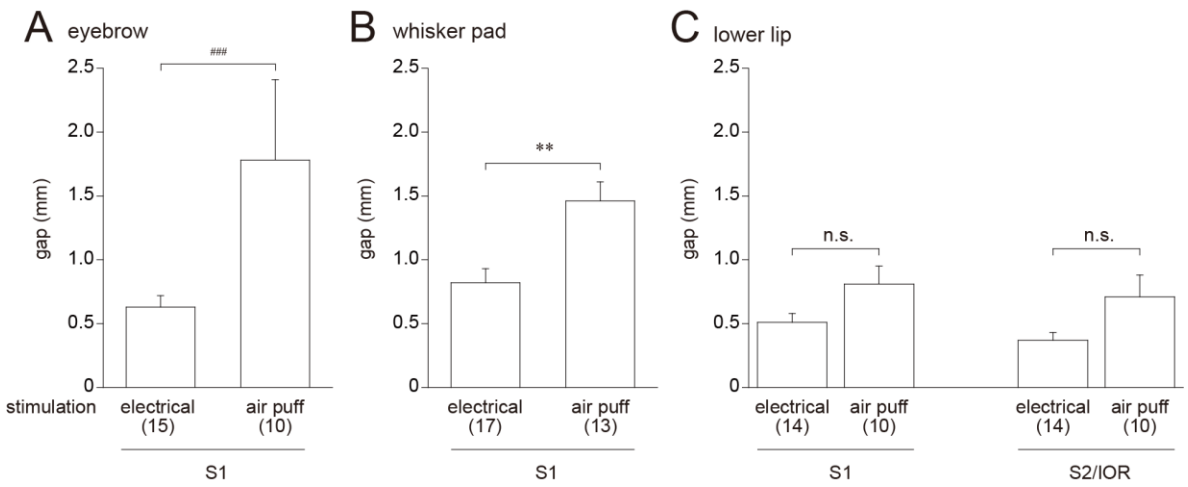

Figure 2. The degrees of scattered initial responses to electrical stimulation and air puff stimulation. (A-C) The gaps between averaged initial response and each initial response to stimulations of the eyebrow (A), whisker pad (B), and lower lip (C) are shown. The numbers of animals are shown in the parenthesis. ** $p <$ 0.01, Student's *t* test; ### $p < 0.001$, Mann–Whitney *U* test; n.s., not significant

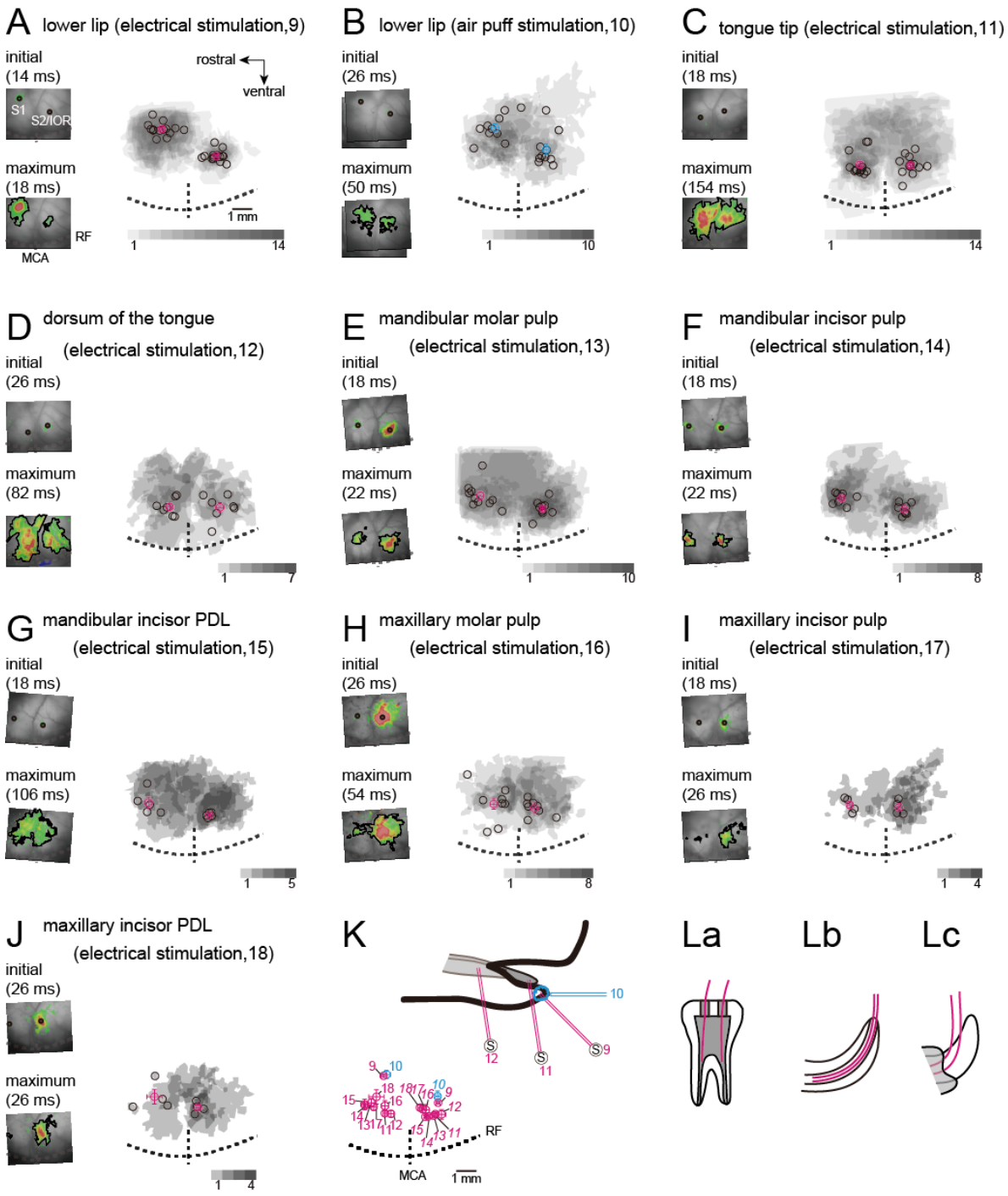

Figure 3. Cortical responses to electrical stimulation and/or air puff stimulation of the oral structures. (A-J) Typical examples of initial and maximum responses to stimulations of the lower lip (A, electrical; B, air puff), tongue tip (C), dorsum of the tongue (D), mandibular molar pulp (E), mandibular incisor pulp (F),

mandibular incisor periodontal ligament (PDL; G), maxillary molar pulp (H), maxillary incisor pulp (I), and maxillary incisor PDL (J) are shown in the left panel in each panel. The time from the onset of stimulation is shown in parenthesis. The initial and maximum responses are superimposed in the right panel in each panel. The magenta (electrical stimulation) or cyan (air puff stimulation) circles and the bars indicate the location of averaged initial responses and SEM, respectively. Each n value is indicated in the scale bar of the density of color. (K) Averaged initial responses in the S1 (regular font) and S2/IOR (italic font) are superimposed using the RF and MCA as references. The numbers correspond to stimulated regions and stimulation methods (A-J, inset). Inset: A schema of stimulated regions and the stimulation methods is shown in the illustration of the oral region. (L) A schema of stimulated teeth was shown. The dental pulp of the 1st molar (La), dental pulp of the incisor (Lb), and PDL of the incisor (Lc) were electrically stimulated by stimulating electrodes (magenta lines).

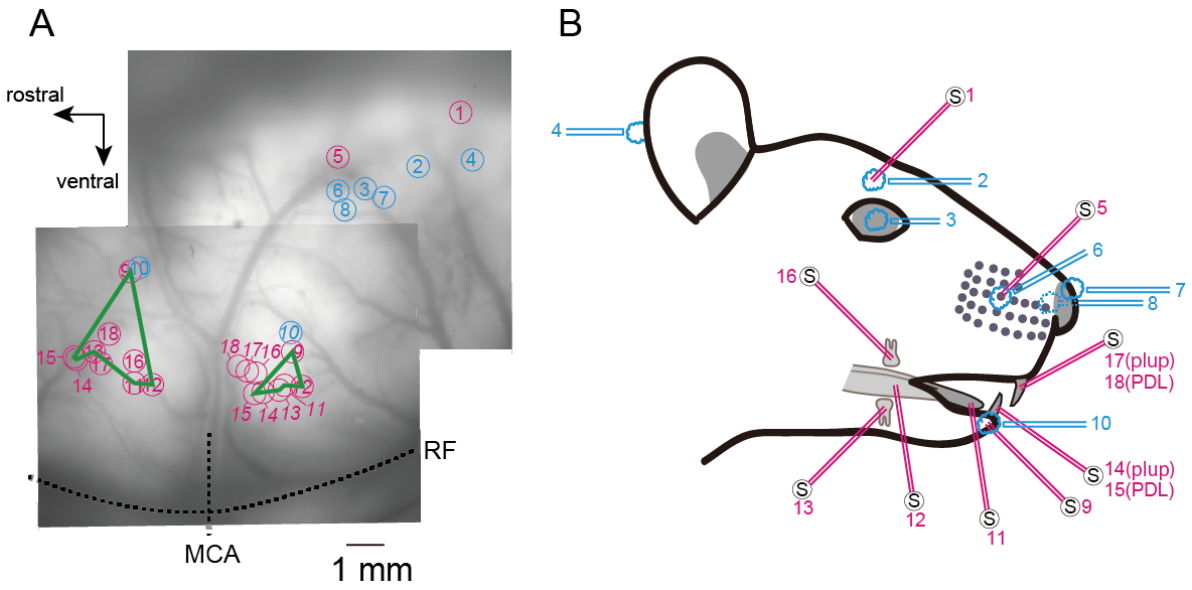

Figure 4. Summary of averaged initial responses. (A) Averaged initial responses in the S1 (regular font) and S2/IOR (italic font) are superimposed using the RF and MCA as references in an example of the cortical surface of a rat. The numbers correspond to stimulated regions (B, Figs. 1 and 3). The green polygons indicate the arrangement of averaged initial responses to electrical stimulation of the lower lip (9), mandibular incisor PDL (15), mandibular incisor pulp (14), mandibular molar pulp (13), tongue tip (11), and dorsum of the tongue (12) in the S1 and S2/IOR. Note that the arrangement of the polygon in the S1 was not inverted in the S2/IOR. (B) A schema of stimulated regions and the stimulation methods is shown. The magenta lines represent electrical stimulation, and the cyan lines represent air puff stimulation. The black circle S indicates electrical stimulation.